에너지공학, 제23권 제4호(2014)
*Journal of Energy Engineering*, Vol. 23, No. 4, pp.112~122(2014)
http://dx.doi.org/10.5855/ENERGY.2014.23.4.112

# The MARS Simulation of the ATLAS Main Steam Line Break Experiment

Tae Wook Ha · Byong Jo Yun · Jae Jun Jeong†
School of Mechanical Engineering, Pusan National University
(Received 25 August 2014, Revised 27 November 2014, Accepted 3 December 2014)

Abstract

A main steam line break (MSLB) test at the ATLAS facility was simulated using the best-estimate thermal-hydraulic system code, MARS-KS. This has been performed as an activity at the third domestic standard problem for code benchmark (DSP-03) that has been organized by Korea Atomic Energy Research Institute (KAERI). The results of the MSLB experiment and the MARS input data prepared for the previous DSP-02 using the ATLAS facility were provided to participants. The preliminary MSLB simulation using the base input data, however, showed unphysical results in the primary-to-secondary heat transfer. To resolve the problems, some improvements were implemented in the MARS input modelling. These include the use of fine meshes for the bottom region of the steam generator secondary side and proper thermal-hydraulics calculation options. Other input model improvements in the heat loss and the flow restrictor models were also made and the results were investigated in detail. From the results of simulations, the limitations and further improvement areas of the MARS code were identified.

**Key words** : Main steam line break, The ATLAS facility, The MARS code, One-dimensional two-phase flow

## 1. Introduction

For a realistic analysis of thermal-hydraulic transients in light water reactors, KAERI has developed the best-estimate system code, MARS [1, 2]. The code has been verified and, thereafter, extensively validated using a wide range of two-phase flow experiments at various facilities, which include a number of both separate effect test and integral effect tests. As a result, the code could have been utilized as a tool for safety analysis and design of nuclear power plants [3 - 5]. The code has been also adopted as an audit calculation tool in the regulatory body. However, there are still many deficiencies in the system codes including the MARS code, especially in the one-dimensional two-phase flow models, such as complicated two-phase flow regimes, interfacial heat/ mass/ momentum transfer, wall heat transfer, and two-phase critical flows. These require continuous improvement of the codes [6, 7].

The DSP exercises using the ATLAS (Advanced Thermal-Hydraulic Test Loop for Accident Simulation) database, led by KAERI, were promoted in order to contribute to improving safety analysis methodology for pressurized water reactors and to transfer the database to domestic nuclear industries [8, 9]. For the first ATLAS DSP exercise (DSP-01), the integral effect test data for a 100% direct vessel injection (DVI) line break accident of the APR1400 was selected [8]. The DSP-03 using the ATLAS MSLB test, was launched on October 9, 2012, after the DSP-02 using the ATLAS small-break loss-of-coolant accident (LOCA) test with a 6-inch break at the cold leg [9]. At the beginning of the DSP-03, KAERI provided the DSP

†To whom corresponding should be addressed.
School of Mechanical Engineering, Pusan National University, Busan, South Korea, 609-735 korea
Tel : 051-510-2455 E-mail : jjjeong@pusan.ac.kr

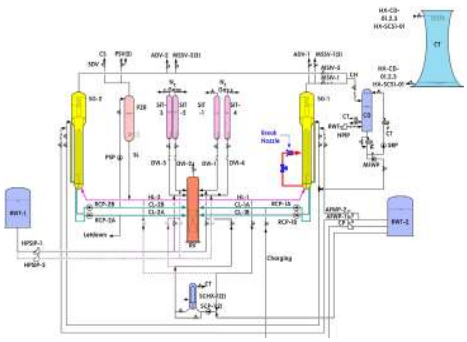

**Fig. 1.** A schematic diagram of the ATLAS [12].

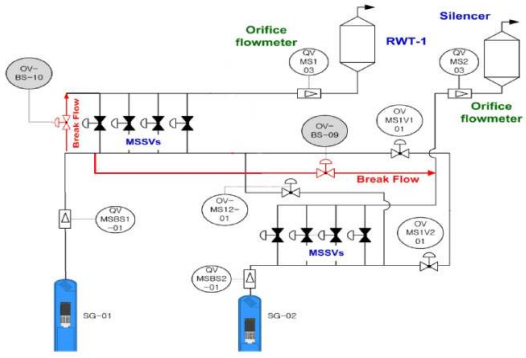


**Fig. 2.** Piping arrangement of the break simulation system [12].

participants with the MSLB test results and the MARS input data for the simulation of a small-break LOCA at the ATLAS, which was established as a result of the DSP-02 activities.

The main objectives of the DSP-03 were to investigate the deficiencies of the existing best-estimate safety analysis codes, to characterize the user effects, and to suggest further code improvement areas. We have participated at the exercise using the MARS-KS code (hereinafter, called MARS). The MSLB simulation based on the MARS input data from the DSP-02 showed some unphysical results in the major parameters, especially in the primary-to-secondary heat transfer. Most of participants, those who used the MARS code, experienced similar problems. It was clear that the input data for the small-break LOCA does not work well for the MSLB simulation. In this study, we have analyzed the MSLB simulation results to find out the reason of unphysical prediction. Some improvements in the input model are suggested. The capability for the ATLAS MSLB simulation, the limitations and further improvement areas of the MARS code are also discussed.

## 2. Description of the ATLAS Facility

The ATLAS experimental facility [10] was designed according to the well-known scaling method suggested by Ishii and Kataoka [11] to simulate various test scenarios as realistically as possible. It is a half-height and 1/288 volume scaled test facility with respect to the APR1400 (Advanced Power Reactor 1400 MWe). The main motive for adopting the reduced-height design is to allow for an integrated annular downcomer, where multi-dimensional flow phenomena can be important in some accident conditions with a DVI operation. According to the scaling law, the reduced height scaling has time reducing results in the model. For the half-height scaled facility, the time for the scaled model is $\sqrt{2}$ times faster than the prototypical time [12].

A schematic diagram of the ATLAS is shown in Fig. 1 [12]. It includes a reactor pressure vessel (RPV), two steam generators, four reactor coolant pumps, a pressurizer, and four safety injection tanks. The ATLAS uses water as the working fluid and is scaled for prototypic pressure and temperature conditions. This selection achieves a fluid property similarity between the APR1400 and the ATLAS in a very simple manner. In order to allow for a simulation of high-pressure scenarios, the loop is designed to operate up to 18.7 MPa.

In the ATLAS test facility, a total of 1,236 instrumentations are installed for the measurement of local thermal-hydraulic conditions, such as temperature, static pressure, differential pressure, water level, flow rate, mass, power, etc. The

uncertainty of measured experimental data is analyzed in accordance with a 95% confidence level. The uncertainty levels of each group of instruments are well described in the literature [13].

## 3. ATLAS MSLB Test

Among a series of the MSLB experiments at the ATLAS facility, the SLB-GB-02T test was chosen in this analysis, which was performed to simulate a double-ended guillotine break accident at the main steam piping located between the outlet nozzle of the steam generator-1 (SG-1) and the corresponding main steam isolation valve (MSIV), OV-MSIV-01 as shown in Fig. 2. In this test, considering the safety analysis results for the MSLB accident of the APR1400 [14], a single-failure of a loss of a diesel generator, resulting in the minimum safety injection flow to the reactor pressure vessel, was assumed to occur in concurrence with the reactor trip. Therefore, the safety injection water from the safety injection pump (SIP) was only available through the DVI-1 and -3 nozzles, and the safety injection water from the safety injection tank (SIT) was available through all of the DVI nozzles. Since the primary system pressure was maintained above the set-point of the SIT, 4.03 MPa during the present MSLB test period, the SIT was not activated.

The break simulation system, presented in Fig. 2, consists of two quick opening valves (OV-BS-09 and -10), break flow discharging lines, flow restrictor, and related instruments including the orifice flow meters to measure the break flow rate. The break flow from the affected SG (SG-1) was directly discharged to a re-fueling water tank (RWT) and the break flow from the intact SG (SG-2) was discharged to the atmosphere through a silencer.

Four main feed water valves (MFIVs) were closed with the opening of the break simulation valves. With the start of the test, the secondary system pressure was decreased rapidly below 6.11 MPa, which is the set-point of the low steam generator pressure (LSGP) signal. With the occurrence of the LSGP signal, the secondary system was isolated with the closure of the MSIVs. The primary pressure also decreased due to the excess heat removal through the secondary side of the SGs. The SIP actuation signal was issued by the low pressurizer pressure (LPP) signal whose set-point is 10.72 MPa. Major event chronology is represented in Table 1.

## 4. Input Model Modification for the MSLB Simulation

The MARS input data prepared for the simulation of a SBLOCA at the ATLAS was used as a base input for the MSLB simulation. With some input modifications for the MSLB simulation, the steady-state condition was obtained and, then, a transient calculation was carried out according to major event chronology listed in Section 3. In general, the results seemed reasonable. However, the transient results showed some unphysical behaviors, especially in the primary-to-secondary

**Table 1.** Major event chronology.

| Time (s) | Event (Remarks) |
|---|---|
| 303 | • Opening of the break valve<br>• Main feedwater isolation signal (coincides with break open) |
| 310 | • Low steam generator dome pressure (LSGP) signal occurred (SG dome pressure < 6.11 MPa) |
| 311 | • RCPs were stopped (LSGP + 1.0 s delay) |
| 315 | • Main steam isolation signal occurred (LSGP + 5.0 s delay) |
| 322 | • Decay power started (LSGP + 12.07 s delay) |
| 364/ 361 | • Auxiliary feedwater actuation signal occurred (SG downcomer water level < 2.78 m + 43.45 s delay) |
| 477 | • Low pressurizer pressure (LPP) signal occurred (Pressurizer dome < 10.721 MPa) |
| 505 | • Safety injection signal occurred (LPP + 28.28 s delay) |

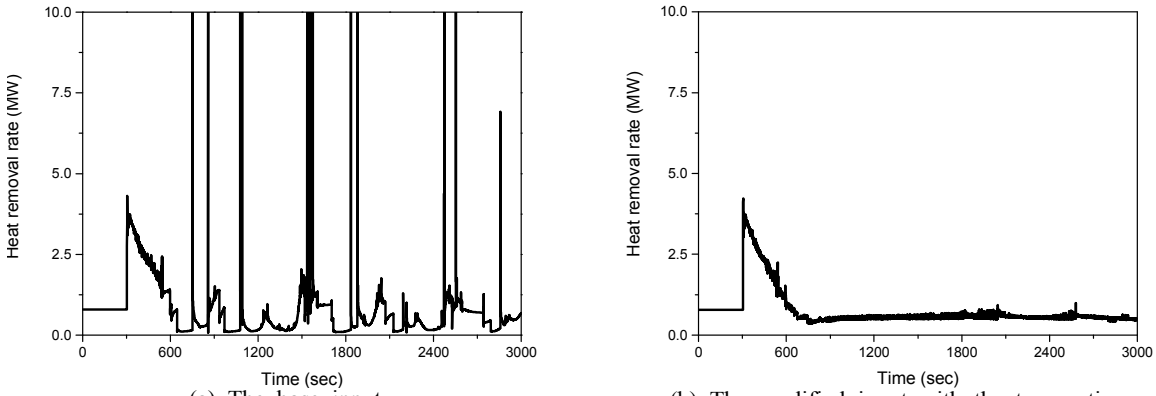


(a) The base input (b) The modified input with the two options

**Fig. 3.** The primary-to-secondary heat transfer at SG-1.

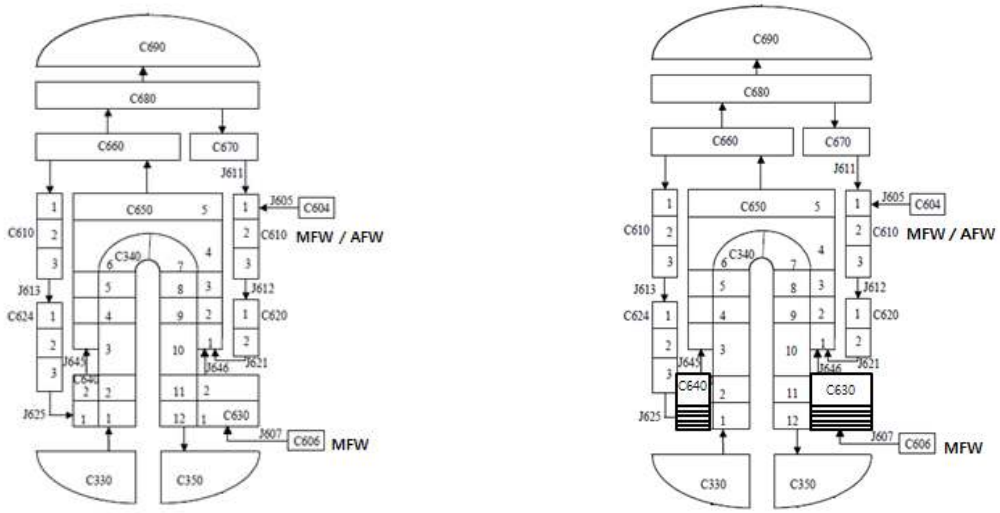


(a) The base input model (b) The modified input model

**Fig. 4.** The SG input model.

heat transfer as shown in Fig. 3 (a). After the MSLB, the coolant of SG-1 is finally depleted and, however, auxiliary feedwater (AFW) is continuously fed into the secondary side of the steam generators. Thereafter, the heat transfer at the lower part of the steam generator tube bundle is unrealistically calculated as depicted in Fig. 3 (a).

Various attempts to solve this problem, i.e., unphysical oscillations in the heat transfer, were conducted. It was found that the discontinuities in two-phase heat transfer model led to this behavior in the secondary side of SG-1 and the use of fine meshes for the bottom region of the steam generator secondary-side improved the result to a great extent. Thus, each of the components 630-1, 640-1, 730-1 and 740-1, representing the bottom region of the SG secondary side, was divided into five equal-sized volumes, as shown in Fig. 4 (b). In addition, the MARS code options 65 and 75 were applied for a smooth transition of boiling flow regimes. These modifications resulted in a more realistic heat transfer in the steam generator, as presented in Fig. 3 (b). The resulting MARS nodalization for the MSLB simulation is presented in Fig. 5.

In addition to the modification of the steam generator input model, the input model for the flow restrictors was added. The flow restrictor, installed at the exit nozzle of the SG, was designed to restrict the maximum mass flow rate from the SG

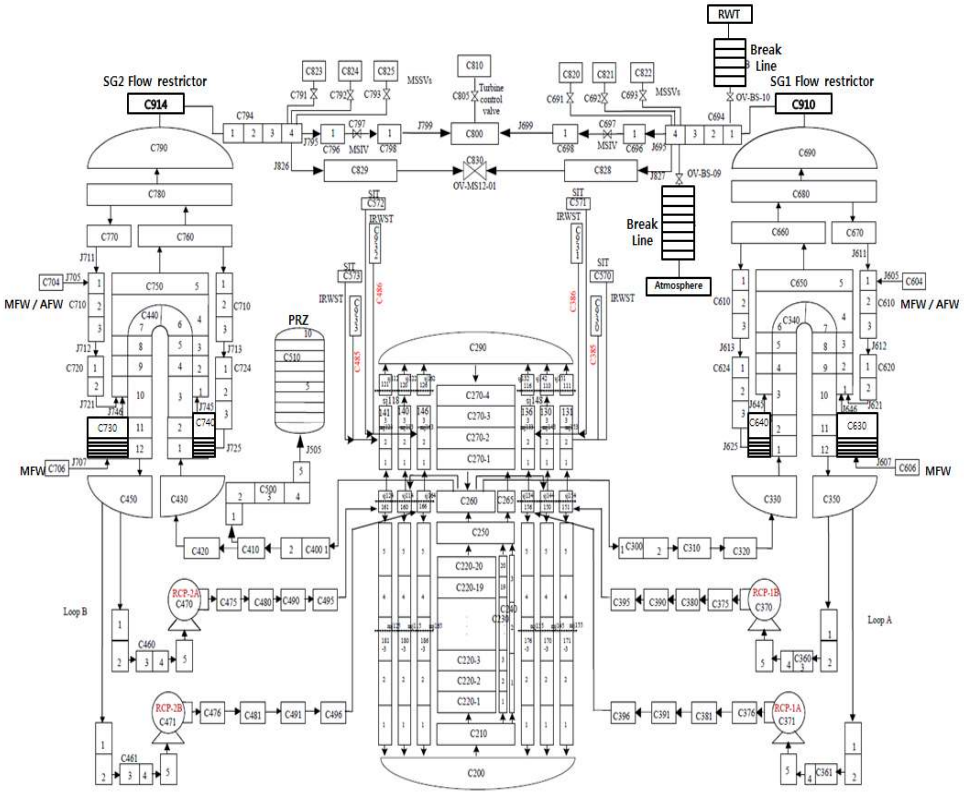


**Fig. 5.** The modified nodalization for the ATLAS.

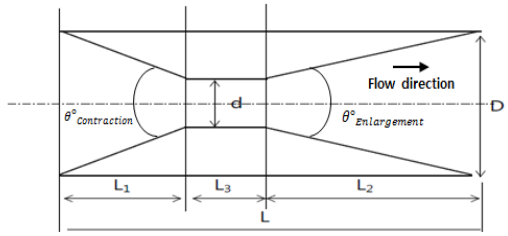


| Type | D | d | L1 | L2 | L3 | L |
|---|---|---|---|---|---|---|
| Choking | 73.0 | 38.6 | 88.48 | 140.07 | 75.63 | 304.18 |
| Non-Choking | 73.0 | 45.9 | 69.70 | 110.34 | 59.58 | 239.62 |

* Unit : mm

**Fig. 6.** The flow restrictor [12].

in the case of a steam line break accident. Because the SLB-GB-02T test was performed to simulate a double-ended guillotine break accident at the main steam piping, the modeling of the flow restrictors is crucial for a realistic simulation. The schematic of the flow restrictor is shown in Fig. 6, which is divided into three sections; contraction ($L_1$), flat ($L_3$), and enlargement ($L_2$). The $L_3$ part is modeled by using a single volume (Components 910 and 914). The $L_1$ and $L_3$ parts are lumped into the up-stream and down-stream volumes, respectively. For the up-stream and down-stream junctions, the following K-factors are given:

$$K = \frac{0.8(\sin\frac{\theta}{2})(1-\beta^2)^2}{\beta^4} \quad (1)$$

for contraction ranging and

$$K = \frac{2.6(\sin\frac{\theta}{2})(1-\beta^2)^2}{\beta^4} \quad (2)$$

for enlargement ranging, where $\beta$ is the ratio of diameters of the small to large pipes and is presented in Fig. 6. Using equations above, the calculated values for K are 1.407 and 2.104, respectively.

Environmental heat losses were also taken into consideration for a better prediction of the MSLB experiment. In this study, the heat losses from the

**Table 2.** Steady state calculation results.

| Parameter | Experiment | MARS | Difference (%) |
|---|---|---|---|
| Primary system | | | |
| Core power (MW) | 1.63 | 1.54* | 0.06 |
| Pressurizer pressure (MPa) | 15.56 | 15.56 | 0.0 |
| Core inlet temperature (K) | 562.75 | 563.34 | 0.10 |
| Core outlet temperature (K) | 567.75 | 567.58 | 0.03 |
| Pressurizer level (m) | 3.21 | 3.21 | 0.0 |
| Cold leg flow rate (kg/s) | 16.4 | 17.3 | 5.5 |
| SIT pressure (MPa) | 4.16 | 4.16 | 0.0 |
| SIT temperature (K) | 323.6 | 323.6 | 0.0 |
| Secondary system | | | |
| SG dome pressure (MPa) | 7.33 / 7.33 | 7.35 / 7.35 | 0.27 / 0.27 |
| SG steam temperature (K) | 564.0 / 564.3 | 562.3 /562.3 | 0.30 / 0.35 |
| Feed water temperature (K) | 507.0 / 505.9 | 506.8 / 505.7 | 0.04 / 0.04 |
| Feed water flow rate (kg/s) | 0.444 / 0.429 | 0.435 / 0.433 | 2.03 / 0.93 |
| SG water level (m) | 5.0 / 5.0 | 5.0 / 5.0 | 0.0 / 0.0 |
| Heat removal (MW) | 0.786 / 0.76 | 0.787 / 0.785 | 0.13 / 3.29 |
| Heat loss rate (kW) | 30 | 28.7 | 4.33 |
| Recirculation ratio | 9.04 / 3.75 | 12.9 / 12.8 | 42.70 / 241.33 |

*Considering heat loss (89.9 kW)

**Table 3.** Sequence of events.

| Event | Experiment (s) | MARS (s) |
|---|---|---|
| Break open | 303 | 303 |
| Main Feedwater Isolation Valve (MFIV) Signal | 303 | 303 |
| Low Steam Generator Pressure (LSGP) Signal | 310 | 307 |
| RCP trip | 311 | 308 |
| Main Steam Isolation Valve (MSIV) Signal | 315 | 312 |
| Decay power started | 322 | 319 |
| Auxiliary Feedwater (AFW) Actuation Signal | 364 | 355 |
| Low Pressurizer Pressure (LPP) Signal | 477 | 470 |
| Safety Injection Pump (SIP) Signal | 505 | 498 |

primary and secondary system were separately modeled. The heat loss at the primary system was considered by decreasing the core power. The secondary heat loss was considered by subtracting the predetermined heat flux from the heat structures for the SGs dome and downcomer (Components 610-3 and 710-3). For each SG, the time-dependent heat losses are specified as a function of time, of which values were measured in experiment [15].

## 5. Results of Simulations and Discussions

Using the modified input model, the steady state was obtained by simulating a null transient of 1,800 seconds. The results are listed in Table 2 and these were used as initial conditions of the transient calculations. In order to achieve the steady-state conditions which are consistent with the experimental data, the steady state controllers were utilized. By these controllers, the core exit temperature and the SG wide-range level were adjusted by manipulating the SG feed water flow rate and reactor coolant pump speed, respectively. In addition, the boundary conditions such as the core power, pressurizer pressure, turbine pressure, were set to the measured initial values. Therefore, almost all parameters has 1% difference between the calculation results and measured values, except the cold leg flow rate, feedwater flow rate, SG heat removal, and heat loss.

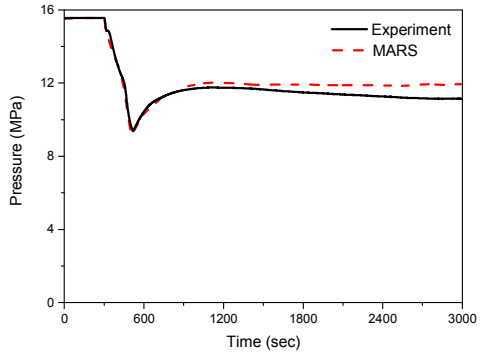


**Fig. 7.** The pressurizer pressure.

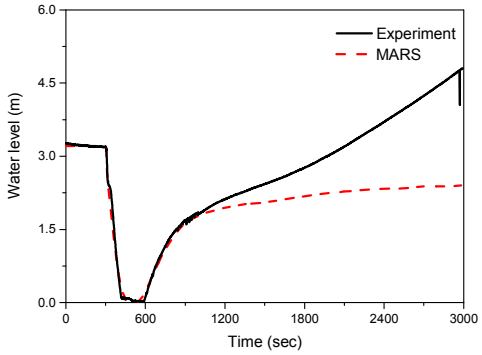


**Fig. 8.** The pressurizer water level.

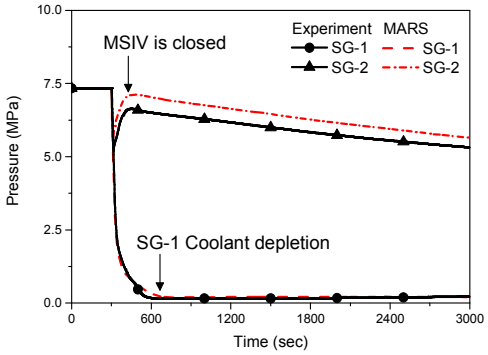


**Fig. 9.** The SG pressure.

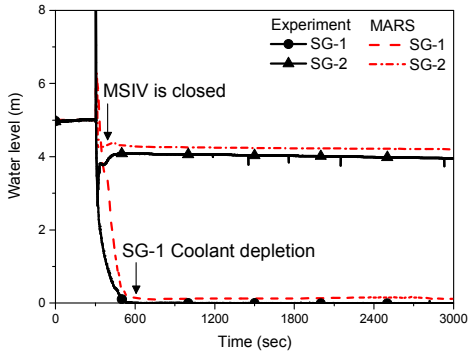


**Fig. 10.** The SG collapsed water level.

Transient calculations were done from the steady-state initial condition. Major sequence of events is compared with the experimental data in Table 3. As shown in Table 3, the chronology of events was well predicted. The major transient parameters are compared with measurements in Figs. 7 ~ 13.

The break opens at 303 s. The predicted pressurizer pressure agrees well with the measured data until 950 s, as can be seen in Fig. 7. However, MARS slightly overpredicts the pressure compared to measured data after 950 s. This overprediction seems to be related to the heat loss of pressurizer dome. Unlike the experiment, adiabatic boundary conditions are applied to the system for MARS calculation. Instead, the primary-side heat loss was simply considered by decreasing the core power. If the steam in the pressurizer dome was condensed by the heat loss, this discrepancy will be decreased.

The pressurizer water collapsed level shows significant deviations with the measured data from 950 s as plotted in Fig. 8, and the discrepancy reaches the maximum ~ 2.4 m in 3000 s. The pressurizer water level may be related to the safety injection flow as well as the coolant temperature. Between the two, the mass flow of SIS may be a dominant factor. The SIS is injected depending on the downcomer pressure. As shown in Fig. 7, MARS significantly overpredicted the pressurizer pressure after the 950 s, resulting in the underprediction of the mass flow rate of SIS. Therefore, the pressurizer water level is underpredicted. However, in the MSLB, the pressurizer water is not a primary concern and, thus, further efforts were not made.

In Fig. 9, the pressure of SG-2 shows a little deviation starting from the time when MSIV is closed. This difference seems to be due to the amount of break flow discharged from SG-2. After MSIV is closed, a slope of SG-2 pressure showed good agreement with the measured data. The overall behavior of SG-1 pressure was predicted relatively well. However, the predicted pressure shows a little deviation at around the time of

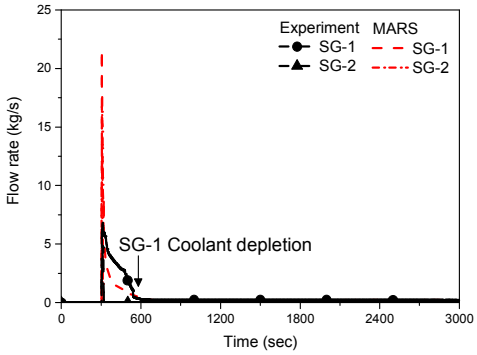


**Fig. 11.** The break flow.

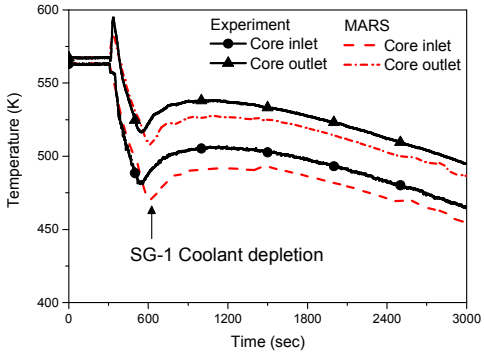


**Fig. 12.** The core inlet and outlet temperatures.

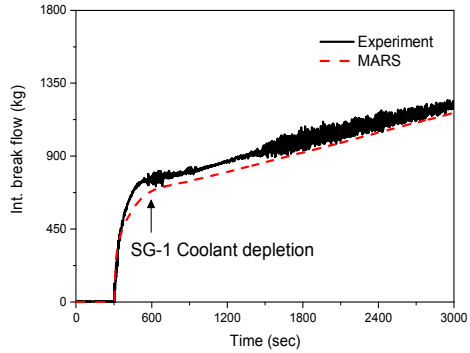


**Fig. 13.** The integrated break flow from the SGs.

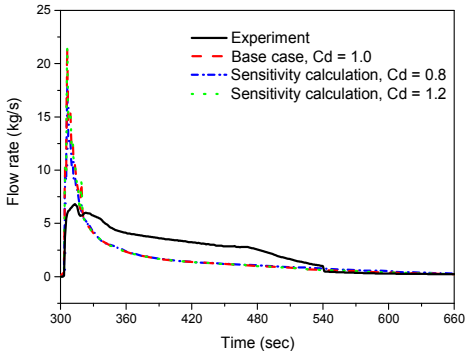


**Fig. 14.** Sensitivity calculation for the break model: break flow.

coolant depletion because of the difference time of coolant depletion.

As shown in Fig. 10, the SG-2 water level shows a slight difference with the measured data after the MSIV is closed. This difference is caused by the amount of integrated break flow of the SG-2 until the closure of MSIV, as mentioned above.

As presented in Fig. 10, the coolant of the SG-1 was depleted at around 560 s in the experiment. On the other hand, the MARS predicted the depletion at around 610 s. After the MSLB, the MARS code predicted that the transition from low-quality to high-quality discharge through the break occurs early compared to the experiment as shown in Fig. 11. Therefore, the break flow was under-predicted after early transient, and the depletion was delayed in the MARS results. The reasons of the delayed depletion are not clear.

As shown in Fig. 11, the calculated break flow shows considerable differences until the depletion of SG-1. The break flow including many droplets and steam was discharged from SG-1 in the earlier transient, and its composition rapidly converted into only steam. In contrast, in the experiment, the break flow including droplets seems to be continuously discharged until the depletion of SG-1. This difference may result from inaccurate prediction of separator performance. As a result, the quality in the SG dome was inaccurately predicted, which affected on the break flow calculation.

The predicted core inlet and outlet temperatures agree well with the measured data until the SG-1 coolant depletion, as shown in Fig. 12. However, the temperatures show significant deviations with the measured data after the SG-1 coolant depletion. The differences are due to the inaccurate prediction of break flow until the depletion.

As presented in Fig. 13, the integrated break flow until 3000 s shows a difference of ~68 kg in comparison with that of the measured data. This difference is caused by two reasons. Firstly, the

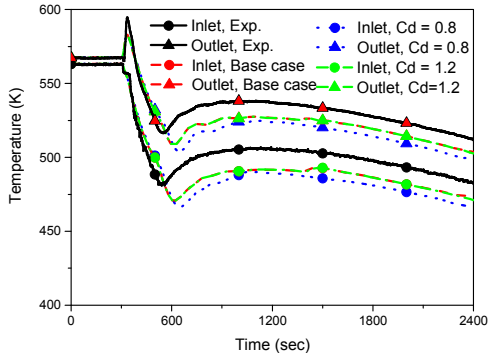


**Fig. 15.** Sensitivity calculation for the break model: the core inlet and outlet temperatures.

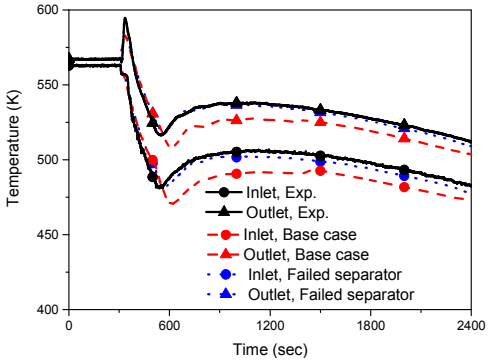


**Fig. 16.** Sensitivity calculation for the separator: the core inlet and outlet temperatures.

collapsed water level of SG-2 is higher than measured data, as shown in Fig. 10. In other words, the break flow seems to be less discharged from SG-2, in the MARS calculation. Secondly, the break flow was measured by using the water level and temperature in the water storage tank, in the experiment. The integrated break flow was calculated by using the measured break flow. However, this measurement may significantly include the uncertainty because only one temperature sensor was used to measure the temperature in water storage tank [16]. Therefore, the integrated break flow shows this difference as shown in Fig. 13.

## 6. Sensitivity Calculations

To improve the MARS results, the input model was carefully reviewed and, then, several sensitivity calculations have been conducted. The two findings are summarized as follows.

### 6-1. Break Flow

The break flow model usually has a great effect on the system transient. However, it was shown that the non-equilibrium factor for the break model did not have a significant effect on the break flow [17]. Therefore, we conducted sensitivity calculations using the default value of 0.14. For the discharge coefficient, we additionally calculated for two cases of 0.8 and 1.2. However, the break flow and core temperature were not significantly improved despite these attempts, as presented in Figs. 14 and 15. This implies that the upstream flow condition is more important than the break flow model itself.

### 6-2. Separator Performance

The separator performance is very important in the case of a MSLB accident because it can determine the quality of steam through the break. In the MARS code, the separator performance is not mechanistically modeled. Instead, the carry-over at the steam outlet and the carry-under at the liquid are specified as user input (0.3 and 0.15 are used as default value, respectively). In this calculation, the default values were used, which seem too ideal for the MSLB transient. For a sensitivity calculation, we just assumed that separators are operated under the worst condition. That is, we assumed no function of the separators. To model this separator, the carry-over parameter was changed to 1.0. Fig. 16 shows the significant effect of the separator performance on the system behaviors. Surprisingly, the depletion time is similar to the experiment because the break flow including more droplets discharges compared to the base case until the depletion. Therefore, the core inlet and outlet temperatures also show a good agreement with measured data. The results indicate the separator performance is very important for the system behaviors.

## 7. Concluding Remarks

As an activity for the DSP-03 exercise, we have simulated the ATLAS MSLB test using the MARS code. The base input data from the DSP-02 small-break LOCA was appropriately modified for the MSLB simulation. From the results of the simulations, the following lessons were drawn.

- MARS unrealistically predicts the SG heat transfer at certain conditions. This may be due to discontinuities in the physical models for the boiling heat transfer curve. This problem could be reduced by using the fine nodalization for the SG and appropriate thermal-hydraulic code options for heat transfer.

- MARS poorly predicted the break flow until the SG-1 coolant depletion. One of the reasons seems to be the uncertainty in the separator model, which affects the upstream condition of the break flow. The break input model itself does not have a significant effect on the transient behaviors in the MSLB simulations.

- The system pressures were significantly related to environment heat loss. In this analysis, the tendency of SG-2 pressure was well predicted. However, the primary pressure shows significant difference because the heat loss from the pressurizer dome was not properly considered. The pressure deviation, in turn, affected the system behavior.

Despite the limitations, it can be said that the MARS code can predict the transient behavior of major parameters during the MSLB accident reasonably well.

## Acknowledgement

This work was supported by a 2-Year Research Grant of Pusan National University.

## References

1. J.J. Jeong, K.S. Ha, B.D. Chung and W.J. Lee, "Development of A Multi-dimensional Thermal-Hydraulic System Code, MARS 1.3.1," Annals of Nuclear Energy, vol. 26, no. 18, pp. 1611-1642 (1999).
2. "MARS code manual volume I: Code structure, System Models, and Solution Methods," Korea Atomic Energy Research Institute, Daejeon & Korea (2009).
3. J.J. Jeong, S.W. Bae, D.H. Hwang, W.J. Lee, and B.D. Chung, "Hot Channel Analysis Capability of the Best-Estimate Multi-Dimensional System Code, MARS 3.0," Nuclear Engineering and Technology, Vol. 37 No.5 pp. 469-478 (2005).
4. Jae Jun Jeong, Seung Wook Lee, Jin Young Cho, Bub Dong Chung, and Gyu-Cheon Lee, " A coupled analysis of system thermal-hydraulics and three-dimensional reactor kinetics for a 12-finger control element assembly drop event in a PWR plant," Annals of Nuclear Energy, 37, 1580-1587 (2010).
5. B.G. Huh, Y.S. Bang, C.Y. Yang, "Best-estimated evaluation for LBLOCA of APR1400 using MARS code," Transactions of the American Nuclear Society, Volume 103, pp. 501-502 (2010).
6. Dominique Bestion and Antoine Guelfi, "Status and Perspective Of Two-Phase Flow Modelling in The Neptune Multiscale Thermal Hydraulic Platform For Nuclear Reactor Simulation, " Nuclear Engineering and Technology, Vol. 37, pp. 511-524 (2005).
7. K.D. Kim, "SPACE Code Development and Improvement," Workshop on Nuclear Safety Analysis Code Development, Korean Nuclear Society, Jeju International Convention Center, May 28, 2014. (in Korean)
8. Yeon-Sik Kim, Ki-Yong Choi, et al., "First ATLAS Domestic Standard Problem (DSP-01) for the Code Assessment," Nuclear Engineering and Technology, Vol. 43, pp.25-44 (2011).
9. Yeon-Sik Kim, Ki-Yong Choi, Seok Cho, Hyun-Sik Park, Kyoung-Ho Kang, Chul-Hwa Song, and Won-Pil Baek, "Second ATLAS Dome

stic Standard Problem (DSP-02) For A Code Assessment," Nuclear Engineering and Technology, Vol.45 No.7, Pp. 871-894 (2013).
10. W.P. Baek, C.H. Song, B.J. Yun, T.S. Kwon, S.K. Moon and S.J. Lee, "KAERI Integral Effect Test Program and the ATLAS Design," Nuclear Technology, Vol. 152, p.183 (2005).
11. M. Ishii and I. Kataoka, "Similarity Analysis and Scaling Criteria for LWRs under Single Phase and Two-Phase Natural Circulation," Argonne National Laboratory, USA (1983).
12. K. H. Kang et al., "Test Report on the Guillotine Break of the Main Steam Line Accident Simulation with the ATLAS," Korea Atomic Energy Research Institute, Daejeon & Korea (2012).
13. K. H. Kang et al., "ATLAS facility and instrumentation description report," Korea Atomic Energy Research Institute, Daejeon & Korea (2009).
14. "KNGR Standard Safety Analysis Report," Chapter 15, Korea Electric Power Corporation, Korea (2005).
15. K. H. Kang et al., "Detailed Description Report of ATLAS Facility and Instrumentation," Korea Atomic Energy Research Institute, Daejeon & Korea (2011).
16. K. Y. Choi, personal communication, June 2014.
17. K. Y. Choi et al., "Comparison Report of Open Calculations for ATLAS Domestic Standard Problem (DSP-02)," Korea Atomic Energy Research Institute, Daejeon & Korea (2011).